Lawrence Berkeley National Laboratory

Title
COLLISION CROSS SECTIONS OF 400 - TO 1800-keV H3+ IONS IN COLLISIONS WITH H2 AND N2 GASES AND Li VAPOR

Permalink
https://escholarship.org/uc/item/6qq8w2zq

Authors
Berkner, K.H.
Morgan, T.J.
Pyle, R.V.
et al.

Publication Date
1973-07-01

COLLISION CROSS SECTIONS OF
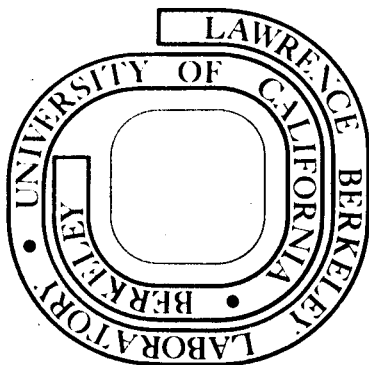## 400- TO 1800-keV H_3^+ IONS IN COLLISIONS WITH H_2 AND N_2 GASES AND Li VAPOR

K. H. Berkner, T. J. Morgan, R. V. Pyle,
and J. W. Stearns

July 1973

DISCLAIMER

COLLISION CROSS SECTIONS OF
400- TO 1800-keV H_3^+ IONS IN COLLISIONS WITH H_2 AND N_2 GASES AND Li VAPOR[*]

K. H. Berkner, T. J. Morgan, R. V. Pyle,
and J. W. Stearns

Lawrence Berkeley Laboratory
University of California
Berkeley, California 94720

July 1973

ABSTRACT

Cross-section measurements of the dissociation modes

$H_3^+ \rightarrow$ (3H and H + H_2), H + H_2^+, H^+ + 2H, H^+ + H_2, H + $2H^+$, H^+ + H_2^+,

and $3H^+$ are reported for H_3^+ energies between 400- and 1800-keV in

targets of H_2, N_2, and Li. For the H_2 target, comparisons are made

with available previous measurements of H, H^+, H_2, and H_2^+ produc-

tion cross sections at lower energies. Cross-section measurements

for 270- to 1200-keV $H_2 \rightarrow H_2^+$, H + H^+, and $2H^+$ are also reported.

I. INTRODUCTION

Elementary interactions of fast H_2^+ ions with gases have been studied in considerable detail, but similar studies of the next molecular hydrogen ion, H_3^+, either experimental or theoretical, apparently have not been reported. A number of experiments are listed below in which cross sections for producing a given interaction product, e.g., H^+ or H, have been deduced. Some measurements of H yield as a function of gas target thickness have also been reported, because of the interest to the controlled nuclear fusion program in ways to make intense neutral beams.

An energetic H_3^+ ion colliding with a target atom or molecule can be destroyed as a result of

(a)	electron capture	$H_3^+ \rightarrow H_3$	(1)
		$H + H_2$	(2)
		$3H$	(3)
(b)	dissociative excitation	$H_3^+ \rightarrow H + H_2^+$	(4)
		$H^+ + 2H$	(5)
		$H^+ + H_2$	(6)
(c)	ionization	$H_3^+ \rightarrow H + 2H^+$	(7)
		$H^+ + H_2^+$	(8)
or (d)	double ionization	$H_3^+ \rightarrow 3H^+.$	(9)
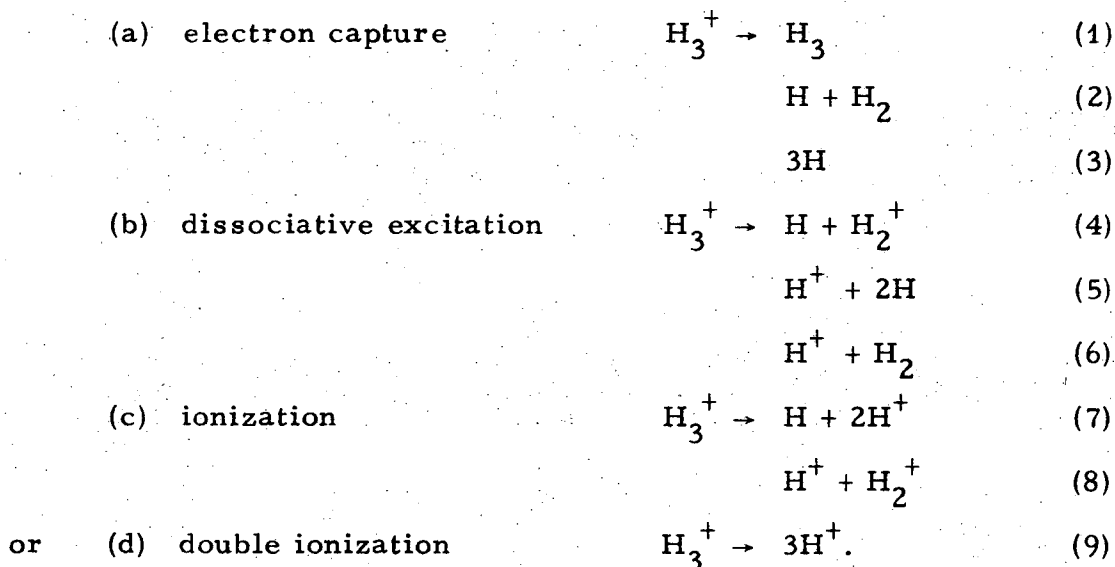
Although potential energy surfaces calculated for the H_3 molecule indicate that there is no stable configuration for the electronic ground state, reaction (1) has been included because highly excited H_3

molecules have been observed experimentally.[1] We have not included reactions which might lead to H^- formation, but we note that Williams and Dunbar[2] have reported cross sections for the production of H^- from H_3^+ in the energy range 2-50 keV. The process of H^- formation is not known.

We have investigated these dissociation modes by pulse-height analyzing the collision fragments and comparing them in coincidence. We have obtained the cross section for electron capture (we could not distinguish the three modes) and cross sections for each of the modes (4)-(6) for 400- to 1800-keV H_3^+ ions colliding with H_2, Li, and N_2.

Of previous measurements reported in the literature[2-19] on the dissociation of H_3^+, those pertinent to this paper are summarized in Table I.[2-12] Most of these cross sections are for the formation of H, H_2, H^+, or H_2^+ and are, therefore, a combination of cross sections for the various modes (1)-(9). To our knowledge there are not previously published measurements for the individual dissociation modes. Sweetman performed such measurements for 1- to 3-MeV H_3^+ in the early 1960's, but these have not been published.[20]

The analysis of the data required a knowledge of cross sections for the reaction $H_2 \rightarrow H + H^+$, $2H^+$, and H_2^+. These cross sections were measured with less precision than those for H_3^+; the results are reported in the Appendix.

II. APPARATUS AND PROCEDURE

The apparatus was similar to that used for measuring dissociation of HeH^+ ions, and the reader is referred to Ref. 21 for details. Energetic H_3^+ ions were produced in a Van de Graaff accelerator equipped with an rf ion source. The ions were momentum analyzed and passed through a gas cell (or oven for the Li target) and the exiting beam and collision fragments were magnetically separated and directed toward an array of four Si surface-barrier detectors. The diameter of the H^+ detector was 2.5 cm; the other detectors, 1 cm. The procedure described in Ref. 21 was used to establish that all reaction products were detected; it was found that the $3H^+$ resulting from double ionization had sufficient transverse energy to require the larger detector in this position.

The pulses from each detector were amplified, shaped, and sorted by pulse height with single-channel analyzers. The products from each of the dissociation modes were identified by comparing the corresponding single-channel analyzer outputs in coincidence. The counting logic is outlined schematically in Fig. 1.

Since the pulse amplitude produced in a Si surface-barrier detector is proportional to the energy deposited in the detector, the two H atoms resulting from reaction (5) registered the same pulse height as the H_2 molecule resulting from reaction (6). It was possible to distinguish between these two processes by installing a retractable screen (several layers of 800-line/cm mesh) with a net transmission of about 1% in front of the neutral detector: The two H atoms

produced by reaction (5) are spatially separated (because of their dissociation energy) and the probability of both atoms penetrating the screen is $\sim 10^{-4}$. Thus by recording the collision fragments both with and without the screen in place, it was possible to distinguish between reactions (5) and (6). A more detailed description of this method and a description of the screen can be found in Ref. 22.

In principle, this method should also allow us to differentiate between reactions (1), (2), and (3); however, the counting rates for the electron-capture fragments were so low that it was impractical to obtain quantitative data at any but the lowest energy.

Two target cells were used: H_2 and N_2 gases were metered into the cell described in Ref. 21. We assign a standard uncertainty of $\pm 7\%$ to the gas target thickness (molecules/cm^2). Lithium vapor was produced in a stainless steel oven with multiple heat shields. The effective length of the target was 4.79 cm; the entrance and exit apertures were 0.254 and 1.09 mm respectively. Resistive heaters were embedded in the stainless steel structure, and chromel-alumel thermocouples immediately above and below the vapor chamber were used to determine the temperature. The thermocouple system was calibrated at 0° and 100° C, and at the melting point of lithium,[23] 180.5 ± 0.5° C. The melting (or solidification) point was identified by a change in a curve of temperature vs time at constant heater power. The data in the compilation by Hultgren et al.[23] were used to convert temperature to vapor pressure. We assign a standard uncertainty of $\pm 12\%$ to the Li-vapor target thickness.

At each energy the analyzer magnet was set to center the beams on the detectors, and the upper- and lower-level discriminators on the single-channel analyzers were set with the aid of a 400-channel pulse-height analyzer. Data were accumulated by counting the pulses from the beam and from all the collision fragments while the gas cell (or Li oven) was maintained at a constant pressure. Measurements were made at 10 to 20 different pressures, from background (approximately 5×10^{-6} Torr) to a pressure which was sufficient to attenuate the incident H_3^+ beam by 10 to 15%.

III. ANALYSIS

The basic method of analysis was the same as that used for HeH^+ (Ref. 21) with four detectors positioned to collect neutrals, H_3^+, H_2^+, and H^+. The total number of incident H_3^+ could be determined by summing the reaction products and adding this sum to the H_3^+ counts, which represented the part of the beam that had suffered no collisions. The sum of the reaction products was independently determined from the coincidence counts and from the individual counts. Any discrepancy alerted us to a loss of particles (due to mis-steering or scattering) or a failure in the coincidence circuits. This was particularly important, since the $3H^+$-producing collisions scattered the products sufficiently to require special care to assure collecting them all.

Once the number of incident H_3^+ was known, the fractions of the beam emerging as H_3^+, $H_2^+ + H^+$, $H_2^+ + H$, $H_2 + H^+$ or $2H + H^+$, $3H$ or

$H_2 + H$, and $3H^+$ were determined at each target pressure. By use of the low-transmission screen the $H_2 + H^+$ and $2H + H^+$ fractions were separated.

From the attenuation of the H_3^+ fraction as a function of target thickness π (the number density of the target gas multiplied by the target length) we obtained the total attenuation cross section σ_T:

$$F_{H_3^+}(\pi) = F_{H_3^+}(\pi = 0) \exp(-\pi\sigma_T), \tag{10}$$

where $F_{H_3^+}(\pi = 0)$ is the fraction of the H_3^+ beam that survives collisions with slits and/or background gas. This fraction was approximately 0.995.

The changes in the fraction of the beam registered in coincidence channel i is

$$dF_i/d\pi = F_{H_3^+}(\pi)\,\sigma_i + \sum_{j \neq i} F_j(\pi)\,\sigma_{ji} - \sum_{j \neq i} F_i(\pi)\,\sigma_{ij}, \tag{11}$$

where σ_i is the cross section for the collision that leads to the set of reaction products registered in channel i and σ_{ij} is an appropriate cross section that would change products registered in channel i to products registered in channel j. For H_2 and N_2 most of the σ_{ij} were obtainable from the literature;[24,25] for Li there is a dirth of cross-section data, and measurements were limited to very thin targets for which the σ_{ij} corrections would be negligible. Cross sections involving collisions of energetic H_2 molecules were not found for any of the targets used; we therefore decided to measure them with a slight

modification of the present apparatus. These measurements are of lower precision than those for H_3^+ and are described in the Appendix.

A numerical scheme was used to obtain the cross sections σ_i from a least-squares fit to Eq. (11). In all but the $3H^+$ case, the summations of Eq. (11) were small compared to the first term, even at the highest pressures used, and mostly served to confirm and improve the accuracy of the results obtained from the "initial growth" portion of the curves. In the case of $3H^+$, however, the population was so small, relative to the other products, that small ionization losses from these products resulted in relatively large additions to the $3H^+$ population. For this reason many of the cross sections for the production of $3H^+$ are quoted with larger errors than the others.

IV. RESULTS

The cross sections obtained from this experiment are given in Table II. The column labeled σ_T lists the total cross section derived from the attenuation of the H_3^+ beam; Σ is the total cross section obtained by summing the partial cross sections. The two should, of course, be equal, and the close agreement of these two numbers gives an internal consistency check of our results. The standard errors are compounded from systematic uncertainties in the target thickness ($\pm 7\%$ for H_2 and N_2 and $\pm 12\%$ for Li), standard deviations of least-squares fits of counts vs target pressure, and run-to-run reproducibility.

The results for the hydrogen target are repeated in graphical form in Fig. 2 to illustrate the energy dependence for the various partial cross sections. The energy dependence is qualitatively similar for the other targets. The cross section for $H_3^+ \rightarrow 3H$, $H_2 + H$ has the steep energy dependence which is characteristic of electron-capture processes.

With the low-transmission screen positioned in front of the neutral detector, no statistically significant counts were observed on the scaler recording pulses produced by three H atoms. Thus, within our detection efficiency, no H_3 molecules were present in our beam. The detection efficiency was such that we should have observed H_3 if more than 0.1% of the electron-capture reactions [(1) + (2) + (3)] proceeded via reaction (1).

Although we could not distinguish between the production of 3H and $H + H_2$, we present the following evidence that most of the electron capture results in $H + H_2$: Only reactions (2) and (6) produce H_2 molecules. We recorded (Fig. 1) the total number of H_2 produced as well as the number of H_2 produced in coincidence with H^+ [reaction (6)] . The difference in these two signals gives the number of H_2 produced in coincidence with H [reaction (2)] . At our lowest energy this difference was equal to the combined 3H and $H + H_2$ signal; thus we conclude that 3H production was negligible with respect to $H + H_2$ production. At the higher energies the difference between H_2 and $H^+ + H_2$ was statistically insignificant and this technique could not be used.

As mentioned in the analysis section, we had to measure H_2 collision cross sections needed in the data reduction. We give the results of these lower-precision measurements in the Appendix.

V. DISCUSSION

Although we have not found any published partial cross-section data for comparison with our results, there are a number of reported measurements of cross sections for production of H, H^+, H_2^+, etc. fragments, mostly for H_3^+ energies less than about 100 keV (Table I). There are also a few measurements of yields of H atoms per H_3^+ in our energy range (these are required for controlled-fusion-experiment design studies).

Cross sections for particle production, obtained from appropriate combinations of the partial cross sections in Table II, are given in Table III. To allow easy comparison with other experimental results, the cross sections for a H_2 target are also given in Figs. 3-6. At lower energies, where there are more measurements, we see a large spread in the reported cross sections. This spread may be due, at least in part, to different excitation distributions of the H_3^+ ion because of different ion-source conditions. Variations with ion-source parameters have been reported in Refs. 2, 6, and 7. (All ion sources were of the rf type, except that Kupriyanov et al.[4] used an electron bombardment source, and McClure,[6] a cold-cathode PIG source.) We did not make a systematic search for such effects, and can only report that in a year's operation with two different Van de Graaff accelerators, no cross-section variations larger than 10% were observed.

In Fig. 7 we show curves of η, the ratio of the number of nuclei emerging as energetic neutral H and H_2 to the number of nuclei in the incident H_3^+ beam. The solid lines have been calculated from the partial cross sections of Table II, the H_2 cross sections given in the Appendix, and σ_{ij} (Sec. III) from Refs. 24 and 25. Direct measurements of η are shown for comparison at 940 keV. An η curve obtained by Middleton et al.[12] at 550 keV is shown for comparison. The consistency of the η data gives some additional confidence in these measurements.

VI. ACKNOWLEDGMENTS

APPENDIX

To make corrections in the growth curves for secondary reactions in H_2 and N_2, it is necessary to know the electron-capture and loss cross sections for H^+, H, H_2^+, and for the dissociation modes for H_2^+ and H_2. Among these, the ionization and dissociation modes for H_2 could not be found in the literature, and it was necessary for us to measure these cross sections.

For convenience, we produced an H_2 beam directly from the H_3^+ beam by admitting gas into the beam line ahead of our apparatus. The charged particles that remained were swept out by installing a large permanent magnet just ahead of the target cell. The resulting beam was 10-20% H_2 molecules, with the rest H atoms. The low transmission screen was used to test for the presence of 2H counts and these were not found, indicating that the collimation at the target cell was sufficient to exclude at least one of all H atoms produced in pairs. No H_3 molecules were seen.

The methods of taking and reducing data were the same as for the rest of the experiment, except that one of the coincidence circuits was changed to measure $H^+ + H$. The 2H yield was not determined. The results are presented in Table A.

Due to the large background of H atoms in the beam, the standard error is estimated to be ±25%, except as otherwise indicated. This was sufficient for our purposes.

Although insufficient data were available to fully correct the Li curves, we did measure the H_2 cross sections in Li as well and include them here.

FOOTNOTES AND REFERENCES

*Work performed under the auspices of the U. S. Atomic Energy Commission.

1. C. F. Barnett and J. A. Ray, Phys. Rev. A $\underline{5}$, 2120 (1972).

2. J. F. Williams and D. N. F. Dunbar, Phys. Rev. $\underline{149}$, 62 (1966).

3. N. V. Fedorenko, Zh. Tekh. Fiz. $\underline{24}$, 769 (1954).

4. S. E. Kupriyanov, A. A. Perov, and N. N. Tunitskii, Zh. Eksp. Teor. Fiz. $\underline{43}$, 763 (1962) [Sov. Phys.-JETP $\underline{16}$, 539 (1963)] .

5. C. F. Barnett, J. A. Ray, and R. M. Warner, Oak Ridge National Laboratory Annual Report ORNL-3472 (1963), p. 60 (unpublished).

6. G. W. McClure, Phys. Rev. $\underline{130}$, 1852 (1963).

7. E. S. Chambers, Phys. Rev. $\underline{139}$, A1068 (1965).

8. F. Bottiglioni, J. Coutant, and E. Gadda, J. Phys. (Paris) $\underline{27}$, 599 (1966).

9. E. S. Solov'ev, R. N. Il'in, and N. V. Fedorenko, Zh. Eksp. Teor. Fiz. $\underline{53}$, 1933 (1967) [Sov. Phys.-JETP $\underline{26}$, 1097 (1968)].

10. C. F. Barnett, M. Rankin, and J. A. Ray, VIe Conference Internationale sur les Phenomenes d'Ionisation dans les Gaz, Paris, 1963, p. 63.

11. B. A. D'yachkov, Zh. Eksp. Teor. Fiz. $\underline{38}$, 1259 (1968) [Sov. Phys.-JETP $\underline{13}$, 1036 (1969)].

12.   C. R. Middleton, M. F. Payne, and A. C. Riviere, J. Phys. B $\underline{4}$, L88 (1971).

13.   N. V. Afrosimov, R. N. Il'in, and N. V. Fedorenko, Zh. Eksp. Teor. Fiz. $\underline{34}$, 1398 (1958) [Sov. Phys.-JETP $\underline{7}$, 968 (1958)].

14.   F. Schwirzke, Z. Physik $\underline{157}$, 510 (1960).

15.   Yu. S. Gordeev and M. N. Panov, Zh. Tekh. Fiz. $\underline{34}$, 857 (1964) [Sov. Phys.-Tech. Phys. $\underline{9}$, 656 (1964)].

16.   D. W. Koopman, J. Chem. Phys. $\underline{49}$, 5203 (1968).

17.   R. H. Hughes, D. B. Kay, C. A. Stigers, and E. D. Stokes, J. Chem. Phys. $\underline{49}$, 2459 (1968).

18.   R. Dagnac, D. Blanc, and D. Molina, Entropie $\underline{30}$, 177 (1969); J. Phys. B $\underline{3}$, 1239 (1970).

19.   F.-Marcel Devienne, C.R. Acad. Sci. (Paris) $\underline{264}$, 1400 (1967).

20.   D. R. Sweetman, UKAEA Culham Laboratory, Culham, Abingdon, U. K., private communication.

21.   J. W. Stearns, K. H. Berkner, R. V. Pyle, B. P. Briegleb, and M. L. Warren, Phys. Rev. A $\underline{4}$, 1960 (1971).

22.   T. J. Morgan, K. H. Berkner, and R. V. Pyle, Phys. Rev. A $\underline{5}$, 1591 (1972).

23.   R. R. Hultgren, R. L. Orr, and K. K. Kelley, unpublished supplement to R. R. Hultgren, R. L. Orr, P. D. Anderson, and K. K. Kelley, Selected Values of Thermodynamic Properties of Metals and Alloys (John Wiley and Sons, Inc., New York, 1963); private communication from R. R. Hultgren, University of California, Berkeley.

24. <u>Atomic and Molecular Collision Cross Sections of Interest in Controlled Thermonuclear Research</u>, Oak Ridge National Laboratory Report ORNL-3113, Revised (1964), unpublished.

25. S. K. Allison and M. Garcia-Munoz, in <u>Atomic and Molecular Processes</u>, edited by D. R. Bates (Academic Press, N. Y., 1962), Chap. 19.

Table I. Summary of published results on the dissociation of H_3^+. Cross sections for the production of H, H_2, H^+, H_2^+, and H^- are denoted by σ_H, σ_{H_2}, σ_{H^+}, $\sigma_{H_2^+}$, and σ_{H^-}. The last three entries in the table refer to papers where yields of dissociation fragments were reported as a function of target thickness.

Authors	Ref.	H_3^+ energy range (keV)	Targets	Cross sections
Fedorenko (1954)	3	5-25	H_2, N_2, Ne, Ar	σ_{H^+}, $\sigma_{H_2^+}$
Kupriyanov et al. (1962)	4	30-100 (D_3^+)	D_2	σ_{D^+}, $\sigma_{D_2^+}$
Barnett et al. (1962)	5	40-200	H_2	σ_{H^+}, $\sigma_{H_2^+}$
McClure (1963)	6	5-120	H_2	σ_{H^+}, $\sigma_{H_2^+}$, σ_H, σ_{H_2}
Chambers (1965)	7	2-55	H_2	σ_{H^+}, $\sigma_{H_2^+}$
Bottiglioni et al. (1966)	8	20-50	Li plasma	σ_{H^+}
Williams and Dunbar (1966)	2	2-50	H_2, He, Ne, Ar	σ_{H^+}, $\sigma_{H_2^+}$, σ_{H^-}
Solov'ev et al. (1967)	9	60-180	H_2, Mg	σ_{H^+}
				Yields of dissociation fragments vs target thickness
Barnett et al. (1963)	10	60-400	H_2, H_2O	H
D'yachkov (1968)	11	100-400	Li	H, H^+, H_2^+, H_3^+
Middleton et al. (1971)	12	410-550	H_2	$H + H_2$, H^+, H_2^+, H_3^+

-17-

Table II. Cross sections for dissociation of H_3^+ (10^{-17} cm^2/molecule). The measured total attenuation cross section is σ_T; the sum of the partial cross sections is Σ.

Target gas	H_3^+ energy (keV)	σ_T	3H and H+H$_2$	H+H$_2^+$	H$^+$+2H	H$^+$+H$_2$	H+2H$^+$	H$^+$+H$_2^+$	3H$^+$	Σ
H$_2$	409	19.5	1.08	2.85	4.90	1.22	6.20	3.01	0.214	19.5
	940	10.4	0.034	1.53	2.22[b]	0.79	4.07	1.58	0.12[b]	10.3
	1800	5.7	0.0026[d]	0.77	1.17	0.61	2.35	0.74	0.037[b]	5.7
Li	400	31.1	0.48	4.4	6.4	2.9	11.0[d]	4.0[e]	0.80[f]	28.8
	900	18.6	0.10[c]	2.7	4.2[c]	1.6[c]	7.6	2.3	0.26[c]	18.7
	1800	11.2	0.015[c]	1.7	2.5	1.1[c]	4.0	1.9	<0.2	11.5
N$_2$	409	67	2.74	7.0	10.7	3.0[b]	26.9	10.2	5.8	66
	940	51	0.227	4.5	6.2	2.6[b]	23.4	8.7	4.8	51
	1800	35	0.031	2.73	5.1	1.94	18.0	5.2	2.26	35

σ for indicated products[a]

[a]Standard errors are ±15% for Li and ±10% for H$_2$ and N$_2$, except as indicated.

[b] ±15%

[c] ±20%

[d] ±25%

[e] ±30%

[f] ±60%

Table III. Cross sections (10^{-17} cm^2/molecule) for the production of the H_3^+-collision fragments H, H_2, H^+, and H_2^+, obtained from appropriate combinations of the entries in Table II. Standard errors are $\pm 15\%$ for Li and $\pm 10\%$ for H_2 and N_2, except as indicated.

Target gas	H_3^+ energy (keV)	σ_H	σ_{H_2}	σ_{H^+}	$\sigma_{H_2^+}$
H_2	409	19.9	2.30	22.2	5.86
	940	10.1	0.82	13.1	3.11
	1800	5.46	0.61	7.33	1.51
Li	400	28.7	3.38	37.7	8.4
	900	18.8	1.70[a]	24.1	5.0
	1800	10.7	1.12[a]	14.1	3.6
N_2	409	58.0	5.74	95.1	17.2
	940	40.5	2.83	78.7	13.2
	1800	31.0	1.97	55.0	7.93

[a] $\pm 20\%$.

Table A.   Cross sections (10^{-17} cm^2/molecule) for the ionization and dissociation of energetic H_2 in H_2, Li, and N_2.   Standard errors are $\pm 25\%$, except as indicated.

Target gas	H_2 energy (keV)	Cross section for indicated product		
		H_2^+	$H + H^+$	$2H^+$
H_2	270	13	<6	<0.6
	600	6.3	2.7	0.2[a]
	1200	3.4	1.9	0.14
Li	270	17	8	1.5[a]
	600	10	6	<1.2
	1200	7	3.5	<0.5
N_2	270	38	<27	<5.8
	600	26	18	3.8
	1200	20	13	2.6

[a] $\pm 40\%$.

FIGURE LEGENDS

Fig. 1. Counting logic: Gates from the single-channel analyzers drove the scalers and the "and" circuits. Each "and" required simultaneous gates from the two sources in order to drive its scaler. The 2H and H_2 counts were distinguished by use of a low-transmission screen placed in front of the neutral detector (see text).

Fig. 2. Collision cross sections for H_3^+ in H_2. Cross sections shown are for the interactions yielding the products shown at the right of each curve. Standard errors are $\pm 10\%$ unless otherwise indicated. Lines are shown only to connect the corresponding data points.

Fig. 3. Cross section for the production of H atoms by collisions of H_3^+ with H_2. Present results, ——; McClure,[6] - - - .

Fig. 4. Cross section for the production of H_2 molecules by collisions of H_3^+ with H_2. Present results, ——; McClure,[6] - - - .

Fig. 5. Cross section for the production of H^+ by collisions of H_3^+ with H_2. Present results, ——; Kupriyanov et al.,[4] K; Fedorenko,[3] F; Chambers[7] (two different ion source conditions), C1 and C2; McClure,[6] M; Barnett, et al.,[5] B; Williams and Dunbar[2] (two different ion source conditions), W1 and W2; Solov'ev, et al.,[9] S.

Fig. 6. Cross section for the production of H_2^+ by collisions of H_3^+ with H_2. See Fig. 5 for explanation of symbols.

Fig. 7. The fraction of the power of an incident H_3^+ beam converted to H and H_2, η, in an H_2 target vs target thickness. The solid lines have been calculated from known cross sections. The ■ are the results of the present experiment; the dashed line is an experimental curve by Middleton, et al. (Ref. 12).
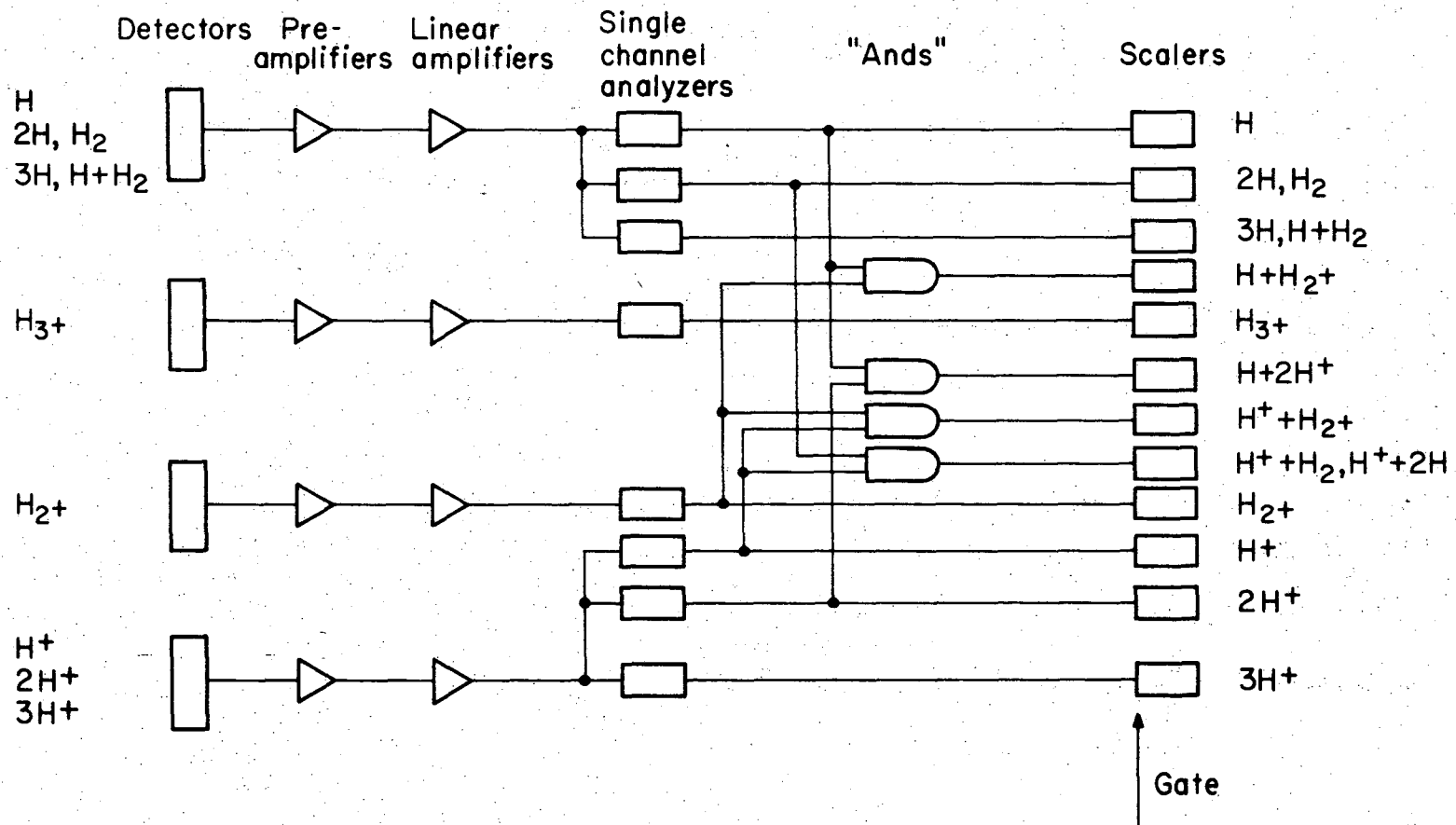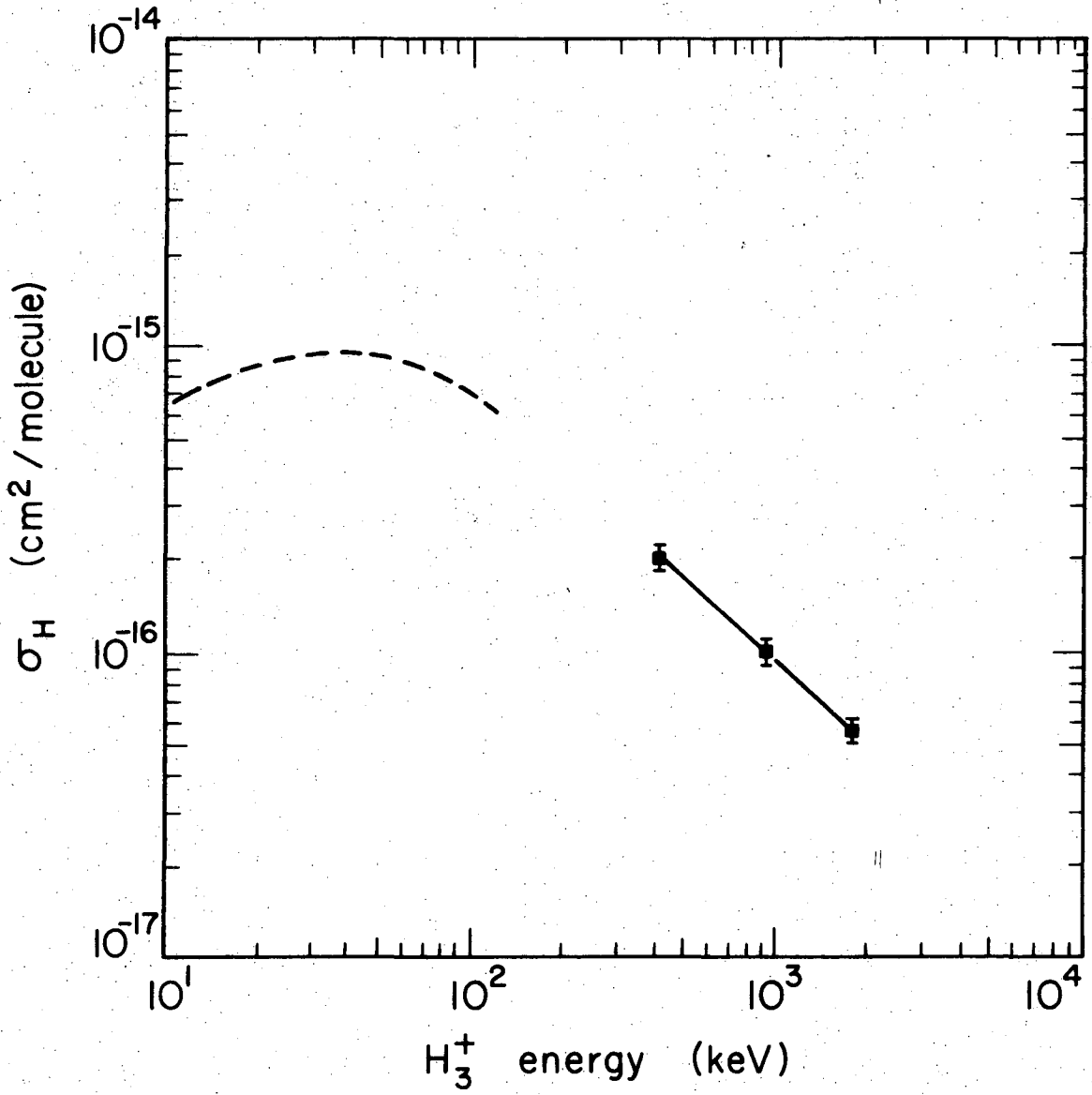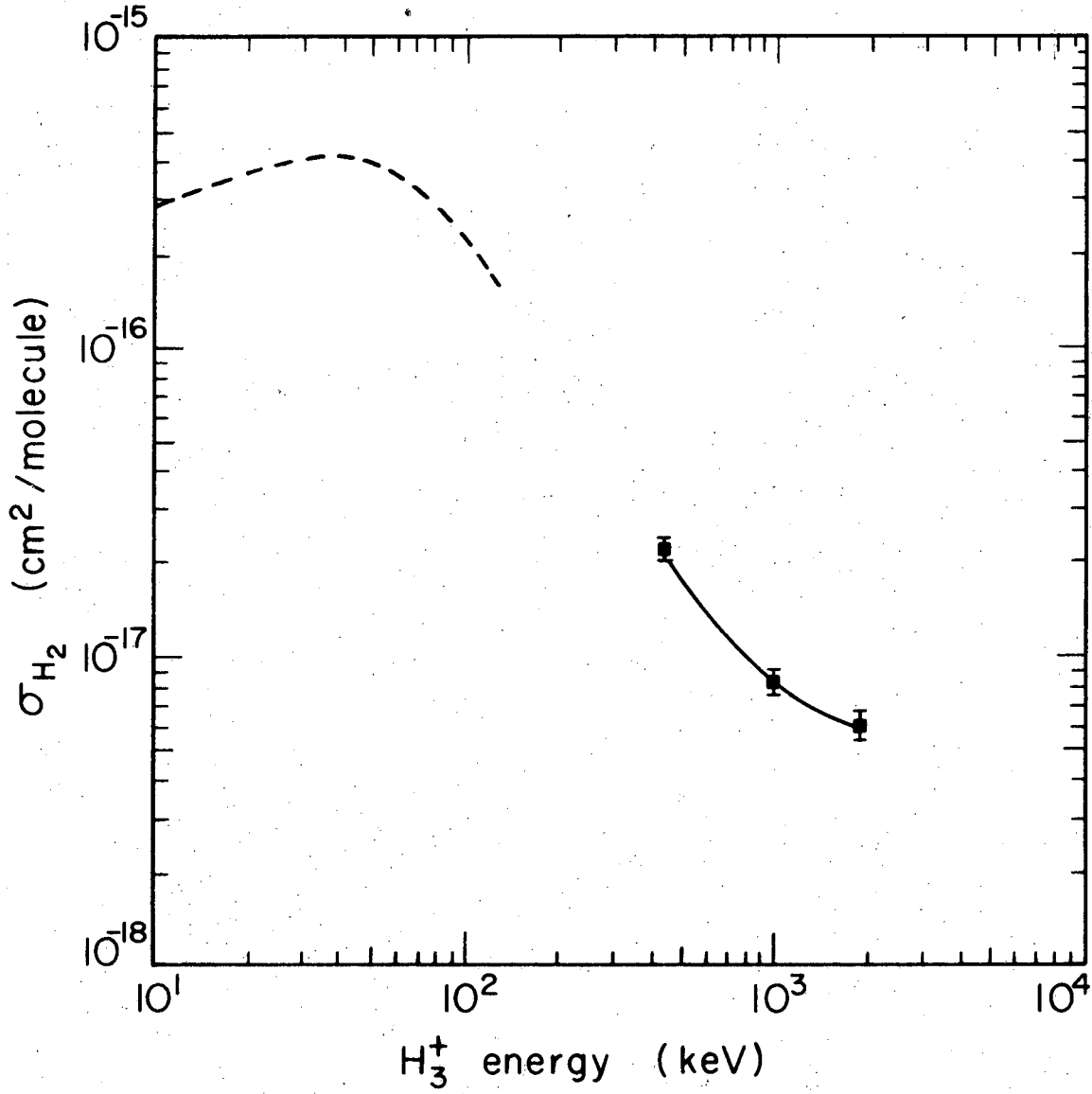
Fig. 1
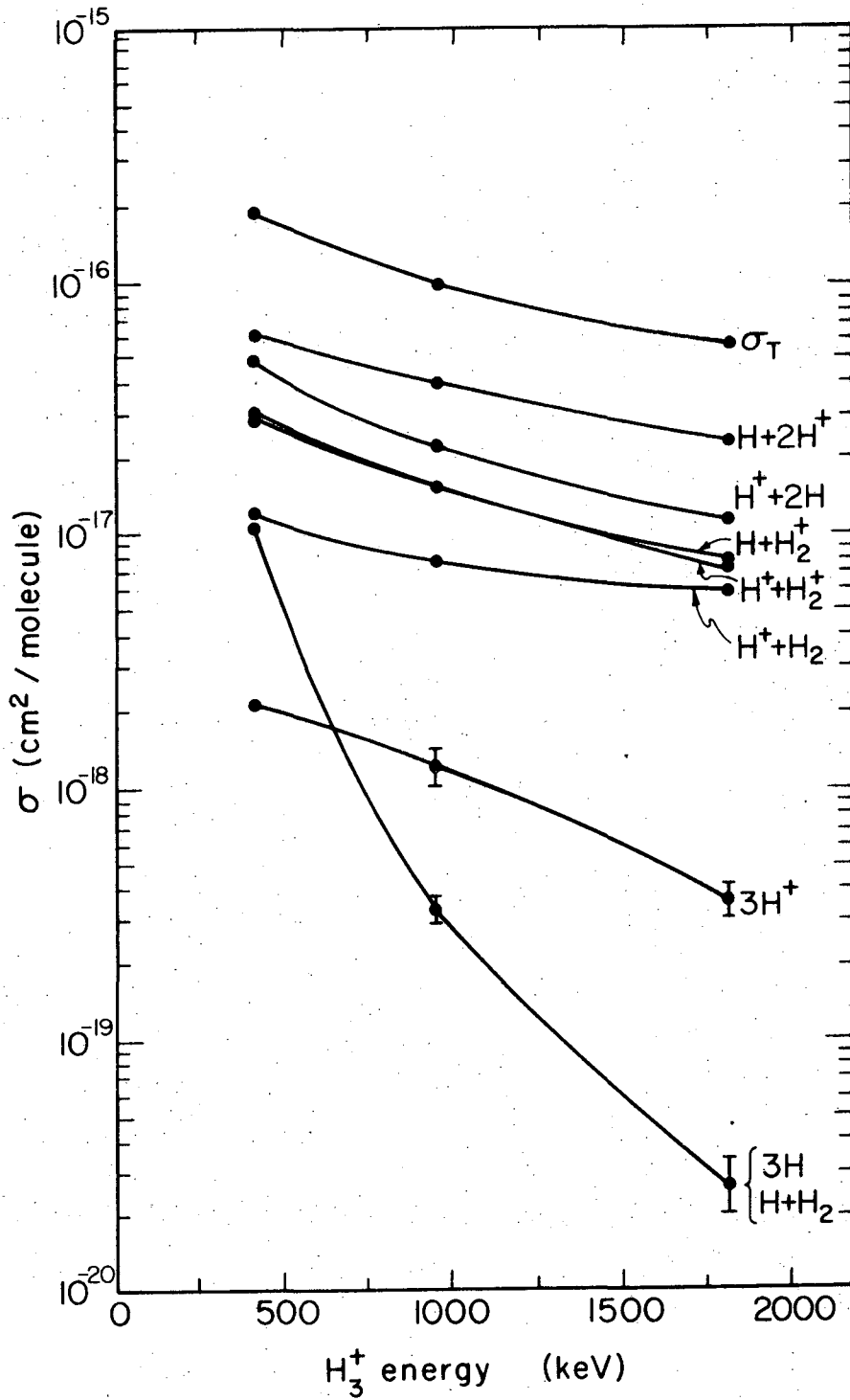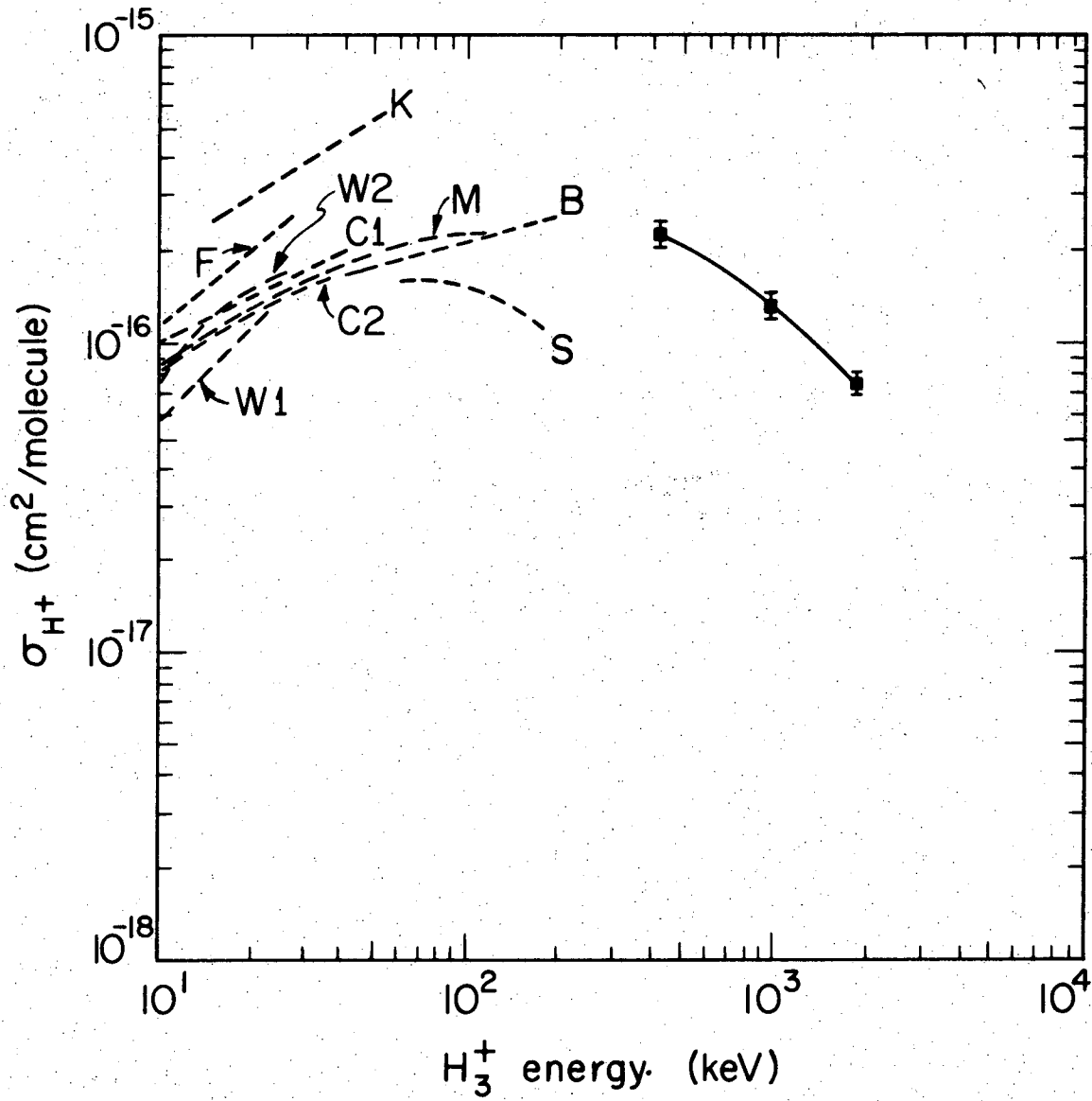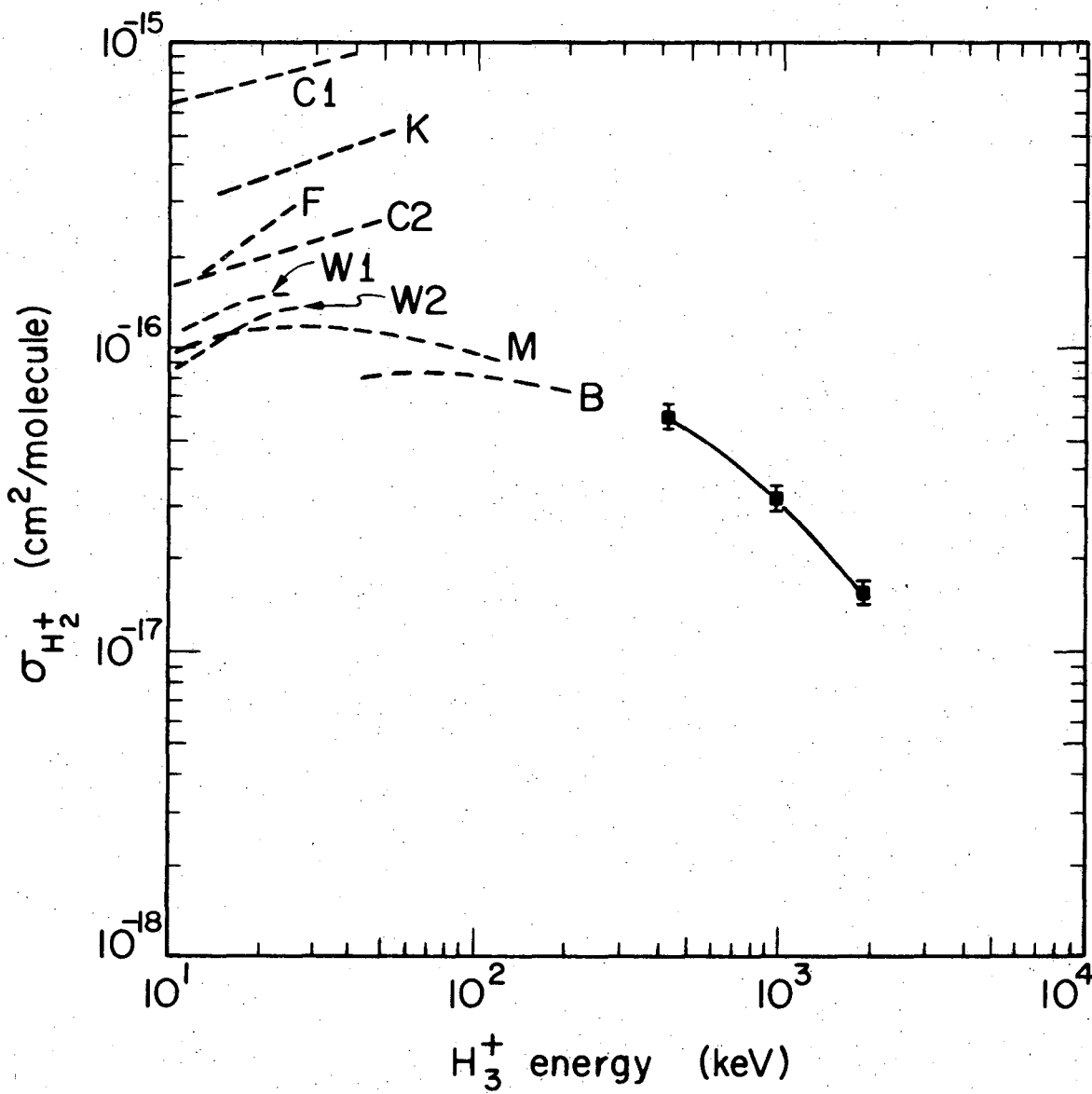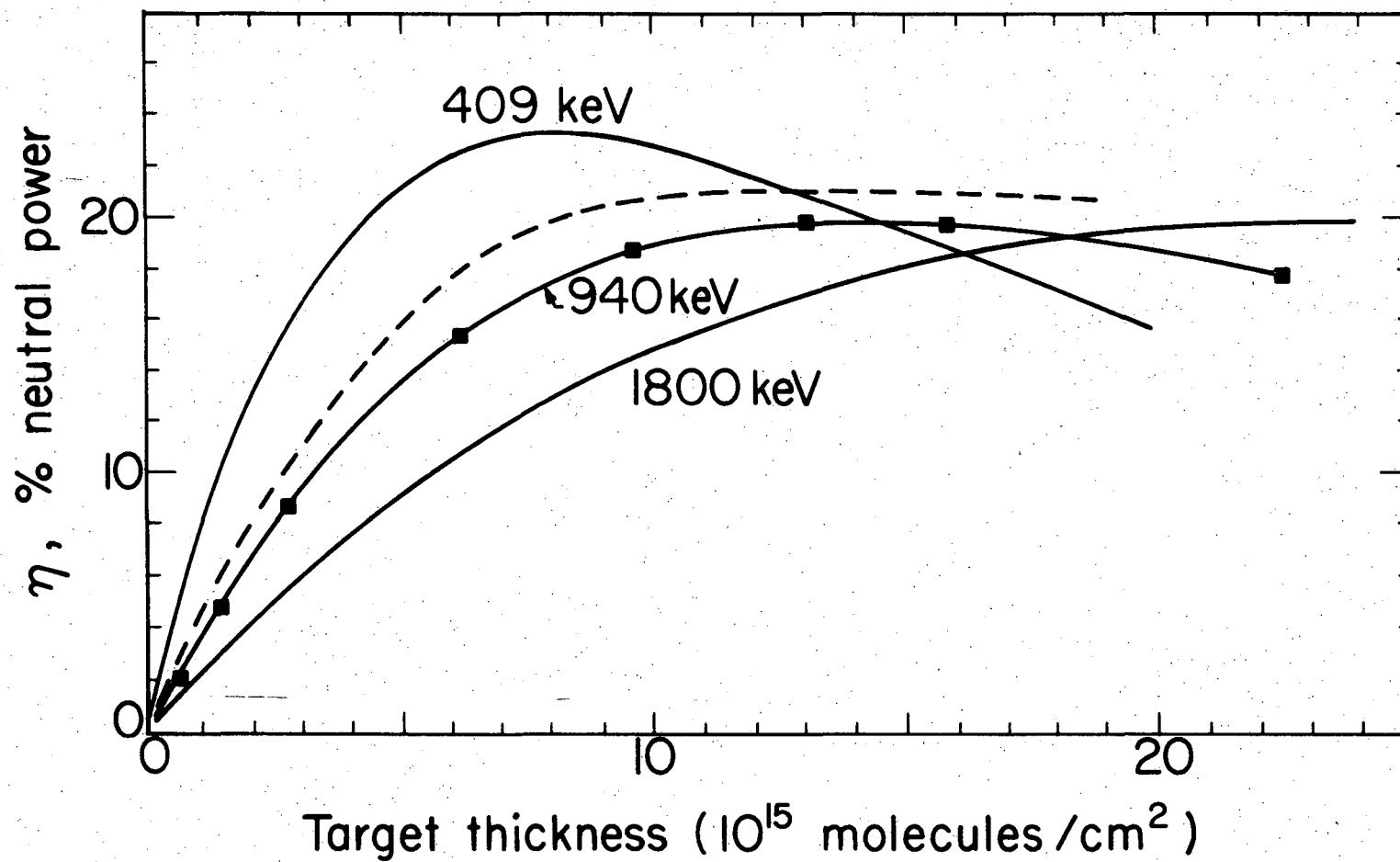
XBL 737-3418

XBL737-3419

Fig. 2

XBL737-3421

Fig. 3

XBL737-3420

Fig. 4

XBL737-3422

Fig. 5

XBL737-3423

Fig. 6

409 keV

20

η, % neutral power

940 keV

1800 keV

10

0

0   10   20

Target thickness (10^{15} molecules/cm^2)

XBL737-3417

Fig. 7